Synthesis of a nanosilica supported CO_2 sorbent ~~by Atomic Layer Deposition~~ in a ~~non-assisted~~ Fluidized Bed Reactor ~~at atmospheric pressure~~

C. Soria–Hoyo[a,*], J. M. Valverde[a], J. R. van Ommen[b], P. E. Sánchez–Jiménez[c], L. A. Pérez–Maqueda[c], M. J. Sayagüés[c]

[a] *Facultad de Física, Universidad de Sevilla, Avda. Reina Mercedes s/n, 41012 Sevilla, SPAIN*

[b] *Department of Chemical Engineering, Delft University of Technology, Product and Process Engineering, Julianalaan 136, 2628 BL Delft, The Netherlands*

[c] *Instituto de Ciencia de Materiales (CSIC - Universidad de Sevilla), Americo Vespucio 49, 41092 Sevilla, SPAIN*

Abstract

CaO has been deposited on a nanosilica powder matrix by **a procedure based on** Atomic Layer Deposition (ALD) in a Fluidized Bed Reactor at atmospheric pressure following a potentially scalable process. In previous works ALD in gas fluidized bed has been mostly performed under reduced pressure, which hampers scaling-up the production technology. The material synthesized in the present work is tested as CO_2 solid sorbent at Calcium Looping conditions. Multicyclic Thermogravimetric analysis (TGA) shows that the nanosilica support stabilizes the capture capacity of CaO. EDX–STEM analysis illustrates the presence of Ca well distributed on the surface of the SiO_2 nanoparticles.

Keywords: ~~Atomic Layer Deposition,~~ Nanosilica, CO_2 sorbent, atmospheric pressure, Calcium looping, Fluidization.

1. Introduction

Calcium-looping (CaL) is a technology based on the multicyclic carbonation of CaO at high temperature and calcination to regenerate the sorbent. The CaL technology is being currently investigated for relevant applications in the energy sector such as postcombustion CO_2 capture[1] and thermochemical storage of concentrated solar power (CSP) using as CaO precursor ~~the~~ widely available and low cost natural limestone ($CaCO_3$)[2, 3].

It is well known that CO_2 chemisorption on CaO derived from natural limestone proceeds through two different phases [4]. A first kinetically–controlled

*Corresponding author. Tel: +34 954559898, fax: +34 954239434
Email address: cshoyo@us.es (C. Soria–Hoyo)

fast reaction phase takes place at the surface of the particle. After a shallow layer (of thickness around 50 nm) is built up on the surface of the particles the reaction continues by a much slower process of diffussion of CO_2 into the bulk of the solid[5]. Only the fast reaction phase is thought to take place in postcombustion capture at practice since the concentration of CO_2 in the flue gases is low and the velocity of the flow is high (on the order of ms^{-1}) leading to short gas–solid residence times. A critical issue of the CaL technology is that the sorbent capacity decays progressively as the number of carb/calc cycles is increased. The drop of capture capacity is particularly marked at postcombustion CO_2 capture conditions[1]. Sorbent deactivation is attributed to the reduction of active surface area by pore sintering at the tipically high calcination temperatures (above 900^o C) and high CO_2 partial pressures in the calciner environment [1]. Silica nanoparticles (NPs) have been coated with CaO in a previous work by capillary impregnation with an aqueous solution of calcium nitrate [6]. The resulting composite showed a stable behaviour as CO_2 sorbent at typical CaL conditions and higher mechanical strength, which was attributed to the stabilizing effect of the silica support.

The present work explores the suitability of Atomic Layer Deposition (ALD) carried out in a Fluidized Bed Reactor (FBR) for coating silica NPs with CaO in order to provide it with a mechanically and thermally stable support. A further purpose of our work will be to demonstrate the feasability of ALD at atmospheric pressure in a non–assisted FBR, which would facilitate the scaling up of this technology with many potential uses in a wide and growing number of applications.

ALD is a technique to deposit thin films of functional materials on substrates [7, 8]. It is based on sequences of self–terminating gas–solid reactions, allowing atomic control of the film thickness [7]. This chemical vapor deposition technique does not require line–of–sight access to the surface, achieving high conformality even on complex shapes [9]. Miniaturization of semiconductor electronic devices has been the main motivation for recent developments in ALD. Yet, it has been also applied successfully to different kinds of substrates [8], such as particles [10], nanomembranes and nanowires [11] and even biological templates [12].

Controlled ALD on particles was developed at the University of Colorado [13, 14, 15]. In regards to particle ALD in a FB it was firstly achieved by Wank *et al.* [16]. Hakim *et al.* [17, 18] extended the technique to NPs-FBR. The first successful application of ALD on particles was achieved by Ferguson *et al.*[19]. Earlier theoretical studies related to ALD can be found in the Eastern literature as well as an experimental work of vanadium layering on coarse silica gel particles in a fixed bed [20]. ALD has been applied to NPs in a FBR at pressures between 1 and 10 Torr achieving completely conformal and pinhole–free coatings [21, 10]. The interested reader may see table II in Longrie *et al.*[22] for a detailed review on ALD in NP–FBRs at reduced pressure. Most of ALD-FBRs currently employed carry precursors into the FBR by an inert gas carrier at low pressures (around 1 Torr). This reduced pressure yields an optimum

balance between the diffusion and entrainment of reactives into the main flow of the inert gas [8, 23].

Application of ALD at atmospheric pressure would usually require long reaction times [8]. The development of efficient ALD in FBRs at atmospheric pressure would be however desirable for scaling-up the functional coating of nano-structured particles from laboratory to industrial applications. Beetstra *et al.*[24] have successfully coated $LiMnO_4$ particles (with typical size from 200 to 500 nm) with Al_2O_3. The precursors were tri-methyl aluminium and water, which is usually considered as close to ideal materials for the ALD process[7]. The resulting coatings were amorphous and their widths showed a dependence with the lattice orientations of the base particles. In a very recent work, ALD in FBRs at atmospheric pressure has been applied to manufacture a relatively large batch size (120 g) of functional aggregates of 200–500 nm $LiMnO_4$ particles coated with Al_2O_3. ALD was carried out in that work by using a FBR assisted by external vibration in order to improve the gas–solid contacting efficiency in the otherwise heterogeneously fluidized bed [25].

In the present paper we show an experimental work aimed at coating aggregates of $\sim$ 10 nm amorphous SiO_2 NPs with CaO in non–assisted FBRs at atmospheric pressure. Nanosilica fluidization properties have been analyzed extensively elsewhere[26]. In contrast with the heterogeneous fluidization behavior exhibited by most nanopowders, nanosilica can be fluidized uniformly by a gas yielding an optimum gas-solid contacting efficency. As will be shown, this allows carrying out ~~ALD~~ the coating in the FBR without the need of external assistance methods, which would be necessary otherwise in order to avoid the likely formation of gas channels and macroscopic bubbles serving as a bypass for the gas flow and thus hampering the ~~ALD~~ coating process. Moreover, low-cost and high purity nanosilica may be easily produced using cheap precursors such as rice husks [27]. **It must be remarked, however, that analyzing the chemistry of the ALD process in the NP-FBR is out of the scopus of the present work, which is mainly focused on demostrating the production of a stable CO_2 sorbent by a potentially scalable technique. Since the self–terminating character of the reactions on the surface of particles will not be assessed it can not be strictly assured that a purely ALD process is taking place. Nevertheless, the self–terminating character of ALD reactions on particles in a FBR has been already demonstrated by King *et al.*[21] by means of *in-situ* mass–spectrometry.**

2. Materials and methods

Two different kinds of nanostructured amorphous silica (commercially available from Evonik) have been used for this study. Aerosil® R974 is an hydrophobic nanosilica powder with average BET area of 150 m^2g^{-1}[28]. Aerosil® 300 has also been employed, which is hydrophilic and has an average BET area of 300 m^2g^{-1}[28]. The precursors used for the ~~ALD~~ **coating** process have been $Ca(thd)_2$ (Bis(2,2,6,6-tetramethyl-3,5-heptanedionato)Ca, from Sigma-Aldrich),

which is a β-diketonate, and O_3. The reactions taking place during the ~~ALD~~ **coating** process would be the following[32]

$$|| - O - H + Ca(thd)_2 \rightarrow || - O - Ca(thd) + H(thd) \quad (1)$$
$$|| - O - Ca(thd) + 20\,O_3 \rightarrow || - Ca - OH + 22\,CO_2 + 19\,H_2O \quad (2)$$

where || denotes the surface of the silica NPs. The net stoichiometry for this set of reactions is thus

$$Ca(thd)_2 + 20\,O_3 \rightarrow CaO + 22\,CO_2 + 19\,H_2O. \quad (3)$$

At the temperature of the reactor CaO and CO_2 will rapidly react to $CaCO_3$.

According to the manufacturer [28], Aerosil 300 has a total density of SiOH groups of about 2.5 groups per nm^2 on its surface with around 1.5 groups per nm^2 isolated and the rest bridged [29]. In the manufacturing of Aerosil R974 the silanol groups have been replaced by dimethylsilyl to make the surface of the NPs hydrophobic [28]. However, a small population of sylanol groups (0.54 groups/nm^2 total, 0.1 isolated groups/nm^2) still remains [29] on the surface.

The area [30] of the $Ca(thd)_2$ molecule ($\simeq 0.87\,nm^2$) imposes a lower limit to the attainable density of a monolayer of this precursor on the surface of the SiO_2 NPs. Taking into account that the curvature of the particles allows for some additional space, the amount of $Ca(thd)_2$ needed to form a monolayer on the surface of a SiO_2 NP would be around 1 molecule/nm^2 . This gives 3×10^{20} molecules, *i.e.* 5×10^{-4} mol or 0.2 g of $Ca(thd)_2$ per gram of SiO_2 NPs. Assuming an ideal gas behaviour for the O_3, and taking into account the stoichiometry of the reaction (eq. 3), the amount of O_3 needed for that purpose would be about $220\,cm^3$. It must be taken into account that the reaction rate r for O_3 decomposition depends on temperature T according to an Arrhenius type law $r \propto \exp(-E/kT)$, where $E > 0$ is the activation energy and R is the ideal gas constant. Thus, at 100° C the O_3 half life is about 12 minutes, while at 250° C the half life drops to just 1 s [31]. Higher temperatures would lead to a very quick decomposition thus severely hampering the ~~ALD~~ **coating** process. Therefore, it is convenient to perform the ~~ALD~~ **coating** cycles at not too high temperature to hinder O_3 decomposition but sufficiently high to favor the vaporization of the solid precursor. For the solid precursor $Ca(thd)_2$, the manufacturer reports a sublimation vapor pressure of 0.1 Torr at 205° C. Thus, a working temperature of 250° C has been chosen as a compromise to avoid O_3 rapid decomposition while, at the same time, achieving a rate of vaporization fast enough to carry out each ~~ALD~~ **coating** cycle in a reasonably short period of time. On the other hand, the temperature of the process could influence the growth–per–cycle. However, at least for a reduced pressure (1.8 mbar), it has been shown that the growth-per-cycle of CaO on SiO_2 is insensitive to temperature within a range of temperatures from 200° C to 400° C [32].

Ten ~~ALD~~ **consecutive coating** cycles have been applied on two samples of nanosilica, one of them consisting of 0.5 g of Aerosil 300 and the other one being 1.0 g for Aerosil R974 both resulting in a surface area of 150 m^2. As

a first step, both Aerosil 300 and R974 samples have been sieved to remove large cohesive agglomerates that may be built up during transport and storage. In each ~~ALD~~ **coating** cycle, the solid precursor if fed from above the FBR (see figure 1) for five minutes after which the bed is purged for 2 minutes by flowing N_2 and subsequently subjected for 5 minutes to a controlled flow of O_2 (previously passed through an ozonizer) followed by other 2 minutes N_2 purging. The flow rates of both N_2 and O_2 were $200\text{cm}^3/\text{min}$. For this value of the gas flow rate, the superficial gas velocity is about 2cm/s which is above the minumum fludization velocity reported for the nanosilica powders used in our study [26, 33].

The dosing and delivery of a solid precursor to the reactor is a critical issue determining in general the efficiency of the ~~ALD~~ coating. With this purpose, diverse techniques have been proposed in the literature [34, 35]. Storing the solid precursor at a high enough temperature to attain a convenient vapor pressure and delivering the vapor to the reactor must be avoided because heating the precursor for long periods may result in its decomposition[35]. The solid precursor used in our work, $Ca(thd)_2$, is a cohesive fine powder. In order to achive a uniform $Ca(thd)_2$ dosing, a mass of 1 g of this cohesive powder has been mixed for 15 minutes in a 20 mm diameter drum at 2 rpm with one thousand 2 mm diameter glass beads. In this process, the $Ca(thd)_2$ fine particles become uniformly adhered to the surface of the carrier glass beads, which allowed us to accurately select of 1 mg doses for ~~ALD~~ precursor direct delivery into the FBR.

Enthaly change ΔH_T^0 for vaporization of many metal β-diketonates (as reviewed by Tsyganova *et al.*[36]) range from 55 to 124 $\text{kJ}\,\text{mol}^{-1}$. Although to our knowledge there are not reported values of ΔH_T^0 for Ca based diketonates we may assume that it should be of the order of 100 $\text{kJ}\,\text{mol}^{-1}$. On the other hand, the flow of heat to $Ca(thd)_2$ on the surface of a carrier glass bead can be calculated as the heat flow to a sphere in a N_2 flow. Expressions for the average Nusselt number $\overline{Nu}_D$ for an isolated sphere submerged in a gas flow are given by Whitaker[37, 38] in terms of the Reynolds ($Re_D = uD/\nu$, where u is the superficial gas velocity, D is the diameter of the sphere and ν is the kinematic gas viscosity) and Prandtl ($Pr = \nu/\alpha$ where α is the thermal diffusivity) numbers. For fluidization of Aerosil, the gas flow velocity is around 1 $\text{cm}\,\text{s}^{-1}$ resulting in Re=0.22 . For these values, the Nusselt number can be estimated[37, 38] as $\overline{Nu}_D \simeq 2$. The ratio of heat flow $\dot{Q}$ to the difference of temperature between the sphere, T, and the surrounding medium, T_m, can be thus calculated from

$$\overline{Nu}_D \equiv \frac{hD}{k} \simeq 2 \tag{4}$$

$$\frac{\dot{Q}}{T - T_m} \simeq h\pi D^2 \simeq 5 \times 10^{-4}\text{WK}^{-1} \tag{5}$$

where h is the heat transfer coefficient and k is the gas thermal conductivity ($k = 41.7 \times 10^{-3}\text{Wm}^{-1}\text{K}^{-1}$). On the other hand, using $\Delta H_T^0 \sim 100\text{kJ}\,\text{mol}^{-1}$, the enthalpy change for 1 mg of $Ca(thd)_2$ is 0.24 J. The difference of temperature $T - T_m$ during the evaporation process varies in time as the $Ca(thd)_2$ evaporates.

Taking into account that at 205°C there is an appreciable value of vapor pressure (0.1 Torr) the difference in temperature during vaporization would be of a few tens of °C, resulting in a vaporization time of the order of tens of seconds.

The experimental setup used in our ~~ALD~~ **coating** experiments is sketched in figure 1. Nanosilica aggregates are suspended in the upwards fluidizing flow of gas inside a 300 mm high and 20 mm internal diameter quartz cylinder(1). A porous quartz plate fitted at the bottom of the tube serves to distribute uniformly the gas flow entering the bed. The fluidized bed is enclosed within a thermostated clamshell furnace (2) which keeps temperature constant at 250° C. Gases entering the fluidized bed are either pure industrial N_2 (99.9% purity) or O_3 carried in the stream of O_2, depending on the phase of the ~~ALD~~ **coating** process. N_2 is pre-heated at 250° C as it passes through stainless steel tubes (3). The N_2 and O_2 flow rates are kept at 200 cm^3/min by means of mass flow controllers (4, 10) (Alicat). A glass flask (5) connects the quartz tube with the gas conduction pipes. This flask is maintained at a constant temperature of 250° C by a heating mantle (6). The solid precursor is manually dosed from the top of the quartz tube through feedthrough (7) directly into the fluidized bed using the carrier glass beads as detailed above. The flow of O_3 is obtained from industrial grade O_2 (99.9% purity) passing through 316L stainless steel tube into a specially designed dielectric-barrier-discharge ozonizer driven by a Trek High Voltage amplifier (50Hz AC 5 kV). The ozonizer yields 15% vol. concentration of O_3. Finally, the gas exits the system through exhaust (11).

3. Results and discussion

Microstructural characterization of the processed samples was performed by means of an analytical TEM-STEM microscope TECNAI G2 F30 (FEI company) with field emission gun (FEG) and point resolution 0.2 nm. The samples were prepared by dispersion of the powder in acetone and droplets of the suspension were deposited onto a coated carbon copper grid. Energy dispersive X-ray spectroscopy (EDX detector, Oxford Instruments) nanoanalysis was performed in STEM mode with a HAADF (High Angle Annular Dark Field) detector and the analysis of the spectra were carried out using a ES Vision software (FEI Company). Images were taken at 300 kV and the micrographs were analyzed with the Digital Micrograph software (Gatan Inc.).

Microstructural and morphological results of the Aerosil 300 processed sample are presented in figure 2. As shown in figures 2b-c the sample consisted of aggregated NPs with an average size of 12 nm (the size distribution is shown in figure 2.a). The different contrast observed in the micrographs can be interpreted in terms of the electronic density, caused either by the difference in thickness of the sample (number of atoms) or by different atoms in different areas (number of electrons per atom). When the electron beam passes through the sample, the contrast is darker where the electron density is higher. At higher magnifications (figure 2.d-e) the micrographs show particles embedded in a matrix of larger particles. Representative results from the chemical analysis are shown in figure 3. The detected amounts of Ca and Si along the line profile

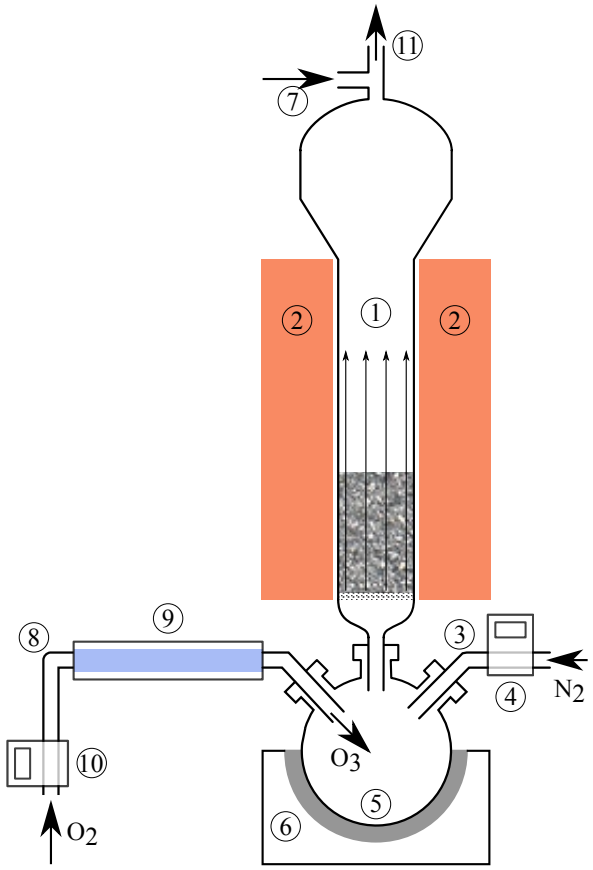

Figure 1: Experimental set-up used for ~~ALD~~ **Ca coating** in a NP-FBR at atmospheric pressure. (1) Quartz tube (300 mm high, 20 mm internal diameter), (2) clamshell furnace, (3) heated steel tubing, (4) mass flow controller, (5) distributor, (6) heating mantle, (7) feedthrough for solid dosing, (8) tubing, (9) ozonizer, (10) mass flow controller and (11) exhaust.

depicted in 3.a are shown in 3.c-d. The relative proportion of Ca is very small, which is consistent with the low number of ~~ALD~~ **coating** cycles to which the samples were subjected (a work under progress is being carried out to automatize the process in order to analyze the effect of increasing the number of cycles). The highest Si/Ca atomic ratio value was found to be 95/5 corresponding to the spectrum displayed in figure 3.b and the position in the image profile marked with a cross.

To test the capacity of the CaO coated materials as CO_2 sorbent, the processed samples have been analyzed by thermogravimetric analysis (TGA) at CaL conditions for post-combustion capture. Samples of about 10 mg were carbonated at 650°C for five minutes in a gas mixture of 85% vol air/ 15% vol CO_2. Carbonation was followed by calcination for five minutes at 950°C in 30%

vol air/ 70% vol CO_2. Carbonation/calcination cycles were carried out using a Q5000IT TG analyzer (TA Instruments) provided with a infrared halogen furnace allowing for a fast heating/cooling rates (300 º C/min) and with a high sensitivity microbalance. The thermograms obtained during the carbonation/calcination cycles are shown in figure 4. TGA tests using pure nanosilica showed no gain/loss of weight upon calcination/carbonation cycles. The results show that the carbonation activity of the ~~ALD~~ synthesized materials remains quite stable after a few cycles, in constrast with the behaviour of limestone derived CaO, which shows a gradual decline of the capture capacity specially marked in the first cycles [6].

4. Conclusions

Nanosilica particles have been successfully coated with CaO ~~by Atomic layer deposition (ALD)~~ in a non–asisted fluidized bed reactor operated at atmospheric pressure and using glass beads as solid precursor carriers directly fed into the fluidized bed. The CO_2 capture capacity of the processed material has been tested in multi–cyclic carbonation/calcination tests. A stable capture capacity is seen during carbonation indicating that nanosilica acts as a thermally stable support to mitigate sintering of CaO in the calcination stages.

Acknowledgements

This work was supported by the Andalusian Regional Government (*Junta de Andalucia*, contracts FQM-5735 and TEP-7858) and Spanish Government Agency *Ministerio de Ciencia e Innovacion* (contracts FIS2011-25161 and CTQ2011-27626).

References

[1] J. Valverde, P. Sanchez-Jimenez, L. Perez-Maqueda, Role of precalcination and regeneration conditions on postcombustion CO_2 capture in the ca-looping technology, Applied Energy 136 (0) (2014) 347 – 356. doi:10.1016/j.apenergy.2014.09.052.
URL http://www.sciencedirect.com/science/article/pii/S0306261914010009

[2] S. E. Edwards, V. Materic, Calcium looping in solar power generation plants, Solar Energy 86 (9) (2012) 2494 – 2503. doi:10.1016/j.solener.2012.05.019.
URL http://www.sciencedirect.com/science/article/pii/S0038092X12001971

[3] G. Flamant, D. Hernandez, C. Bonet, J. Traverse, Experimental aspects of the thermochemical conversion of solar-energy -decarbonation of $CaCO_3$, Solar Energy 24 (4) (1980) 385–395. doi:10.1016/0038-092X(80)90301-1.

[4] J. M. Valverde, Ca-based synthetic materials with enhanced CO_2 capture efficiency, J. Mater. Chem. A 1 (2013) 447–468. doi:10.1039/C2TA00096B.
URL http://dx.doi.org/10.1039/C2TA00096B

[5] G. Grasa, R. Murillo, M. Alonso, J. C. Abanades, Application of the random pore model to the carbonation cyclic reaction, AIChE Journal 55 (5) (2009) 1246–1255. doi:10.1002/aic.11746.
URL http://dx.doi.org/10.1002/aic.11746

[6] P. Sánchez-Jimenez, L. Perez-Maqueda, J. Valverde, Nanosilica supported cao: A regenerable and mechanically hard CO_2 sorbent at ca-looping conditions, Applied Energy 118 (0) (2014) 92 – 99. doi:10.1016/j.apenergy.2013.12.024.
URL http://www.sciencedirect.com/science/article/pii/S0306261913010234

[7] R. L. Puurunen, Surface chemistry of atomic layer deposition: A case study for the trimethylaluminum/water process, Journal of Applied Physics 97 (12) (2005) –. doi:10.1063/1.1940727.
URL http://scitation.aip.org/content/aip/journal/jap/97/12/10.1063/1.1940727

[8] S. M. George, Atomic Layer Deposition: An Overview, Chemical Reviews 110 (1) (2010) 111–131. doi:10.1021/cr900056b.

[9] C. Detavernier, J. Dendooven, S. Pulinthanathu Sree, K. F. Ludwig, J. A. Martens, Tailoring nanoporous materials by atomic layer deposition, Chem. Soc. Rev. 40 (2011) 5242–5253. doi:10.1039/C1CS15091J.
URL http://dx.doi.org/10.1039/C1CS15091J

[10] D. M. King, X. Liang, A. W. Weimer, Functionalization of fine particles using atomic and molecular layer deposition, Powder Technology 221 (SI) (2012) 13–25. doi:10.1016/j.powtec.2011.12.020.

[11] C. Marichy, M. Bechelany, N. Pinna, Atomic layer deposition of nanostructured materials for energy and environmental applications, Advanced Materials 24 (8) (2012) 1017–1032. doi:10.1002/adma.201104129.
URL http://dx.doi.org/10.1002/adma.201104129

[12] M. Knez, A. Kadri, C. Wege, U. Gosele, H. Jeske, K. Nielsch, Atomic layer deposition on biological macromolecules: Metal oxide coating of tobacco mosaic virus and ferritin, Nano Letters 6 (6) (2006) 1172–1177. doi:10.1021/nl060413j.

[13] S. George, J. Ferguson, A. Weimer, Atomic layer controlled deposition on particle surfaces, US Patent 6,613,383 (2003).

[14] S. George, J. Ferguson, A. Weimer, J. Wank, Insulating and functionalizing fine metal-containing particles with conformal ultra-thin films, US Patent 6,713,177 (2004).

[15] S. George, J. Ferguson, A. Weimer, J. Wank, Nanocoated primary particles and method for their manufacture, US Patent 6,913,827 (2005).

[16] J. Wank, S. George, A. Weimer, Nanocoating individual cohesive boron nitride particles in a fluidized bed by ALD, Powder Technology 142 (1) (2004) 59–69. doi:10.1016/j.powtec.2004.03.010.

[17] L. Hakim, J. Blackson, S. George, A. Weimer, Nanocoating individual silica nanoparticles by atomic layer deposition in a fluidized bed reactor, Chemical Vapor Deposition 11 (10) (2005) 420–425. doi:10.1002/cvde.200506392.

[18] L. Hakim, S. George, A. Weimer, Conformal nanocoating of zirconia nanoparticles by atomic layer deposition in a fluidized bed reactor, Nanotechnology 16 (7, SI) (2005) S375–S381, 4th Topical Conference on Nanoscale Science and Engineering of the American-Institute-of-Chemical-Engineers, Austin, TX, NOV 07-12, 2004. doi:10.1088/0957-4484/16/7/010.

[19] J. Ferguson, A. Weimer, S. George, Atomic layer deposition of ultrathin and conformal Al2O3 films on BN particles, Thin Solid Films 371 (1-2) (2000) 95–104. doi:10.1016/S0040-6090(00)00973-1.

[20] S. Yakovlev, A. Malygin, S. Koltsov, V. Aleskovskii, Y. Chesnokov, I. Protodyakonov, Matematical model of molecular layering with the aid of a fluidized bed, Journal of Applied Chemistry of the USSR 52 (5) (1979) 959–963.

[21] D. M. King, J. A. Spencer, II, X. Liang, L. F. Hakim, A. W. Weimer, Atomic layer deposition on particles using a fluidized bed reactor with in situ mass spectrometry, Surface & Coatings Technology 201 (22-23) (2007) 9163–9171, 16th European Conference on Chemical Vapor Deposition, Hague, Netherlands, sep 16-21, 2007. doi:10.1016/j.surfcoat.2007.05.002.

[22] D. Longrie, D. Deduytsche, C. Detavernier, Reactor concepts for atomic layer deposition on agitated particles: A review, Journal of Vacuum Science & Technology A 32 (1) (2014) 010802. doi:10.1116/1.4851676.
URL http://scitation.aip.org/content/avs/journal/jvsta/32/1/10.1116/1.4851676

[23] J. S. Jur, G. N. Parsons, Atomic Layer Deposition of Al2O3 and ZnO at Atmospheric Pressure in a Flow Tube Reactor, ACS Applied Materials & Interfaces 3 (2) (2011) 299–308. doi:10.1021/am100940g.

[24] R. Beetstra, U. Lafont, J. Nijenhuis, E. M. Kelder, J. R. van Ommen, Atmospheric Pressure Process for Coating Particles Using Atomic Layer Deposition, Chemical Vapor Deposition 15 (7-9) (2009) 227–233. doi:10.1002/cvde.200906775.

[25] A. Goulas, J. R. van Ommen, Scalable production of nanostructured particles using atomic layer deposition, KONA Powder and Particle Journal 31 (2014) 234–246. doi:10.14356/kona.2014013.

[26] C. Zhu, Q. Yu, R. Dave, R. Pfeffer, Gas fluidization characteristics of nanoparticle agglomerates, AIChE Journal 51 (2) (2005) 426–439. doi:10.1002/aic.10319.

[27] C. Real, M. Alcala, J. Criado, Preparation of silica from rice husks, Journal of the American Ceramic Society 79 (8) (1996) 2012–2016. doi:10.1111/j.1151-2916.1996.tb08931.x.

[28] Evonik Industries, Basic characteristics of AEROSIL fumed silica. Technical Bulletin Fine Particles 11, 4th ed. Degussa.

[29] J. Mathias, G. Wannemacher, Basic characteristics and applications of aerosil: 30. the chemistry and physics of the aerosil surface, Journal of Colloid and Interface Science 125 (1) (1988) 61 – 68. doi:10.1016/0021-9797(88)90054-9.
URL http://www.sciencedirect.com/science/article/pii/0021979788900549

[30] E. Lakomaa, Atomic Layer Epitaxy (ALE) on porous substrates, Applied Surface Science 75 (1994) 185–196, 2nd International Symp on Atomically Controlled Surfaces and Interfaces (ACSI-2), Joensuu, Finland, jun 16-18, 1993. doi:10.1016/0169-4332(94)90158-9.

[31] J. Heimerl, T. Coffee, The unimolecular ozone decomposition reaction, Combustion and Flame 35 (0) (1979) 117 – 123. doi:10.1016/0010-2180(79)90015-4.
URL http://www.sciencedirect.com/science/article/pii/0010218079900154

[32] O. Nilsen, H. Fjellvag, A. Kjekshus, Growth of calcium carbonate by the atomic layer chemical vapour deposition technique, Thin Solid Films 450 (2) (2004) 240–247. doi:10.1016/j.tsf.2003.10.152.

[33] W. Yao, G. Guangsheng, W. Fei, W. Jun, Fluidization and agglomerate structure of SiO_2 nanoparticles, Powder Technology 124 (12) (2002) 152 – 159. doi:10.1016/S0032-5910(01)00491-0.
URL http://www.sciencedirect.com/science/article/pii/S0032591001004910

[34] R. Hiskes, S. Dicarolis, J. Young, S. Laderman, R. Jacowitz, R. Taber, Single source metalorganic chemical vapor-deposition of low microwave surface-resistance $YBA_2CU_3O_7$, Applied Physics Letters 59 (5) (1991) 606–607. doi:10.1063/1.105400.

[35] P. O'Brien, N. Pickett, D. Otway, Developments in CVD delivery systems: A chemist's perspective on the chemical and physical interactions between precursors, Chemical Vapor Deposition 8 (6) (2002) 237–249. doi:10.1002/1521-3862(20021203)8:6<237::AID-CVDE237>3.0.CO;2-O.

[36] E. I. Tsyganova, L. M. Dyagileva, The reactivity of metal β-diketonates in the thermal decomposition reaction, Russian Chemical Reviews 65 (4) (1996) 315.
URL http://stacks.iop.org/0036-021X/65/i=4/a=R03

[37] S. Whitaker, Forced convection heat transfer correlations for flow in pipes, past flat plates, single cylinders, single spheres, and for flow in packed beds and tube bundles, AIChE Journal 18 (2) (1972) 361–371. doi:10.1002/aic.690180219.
URL http://dx.doi.org/10.1002/aic.690180219

[38] T. L. Bergman, A. S. Lavine, F. P. Incropera, D. P. Dewitt, Fundamentals of Heat and Mass Transfer, John Wiley & Sons, 2011.

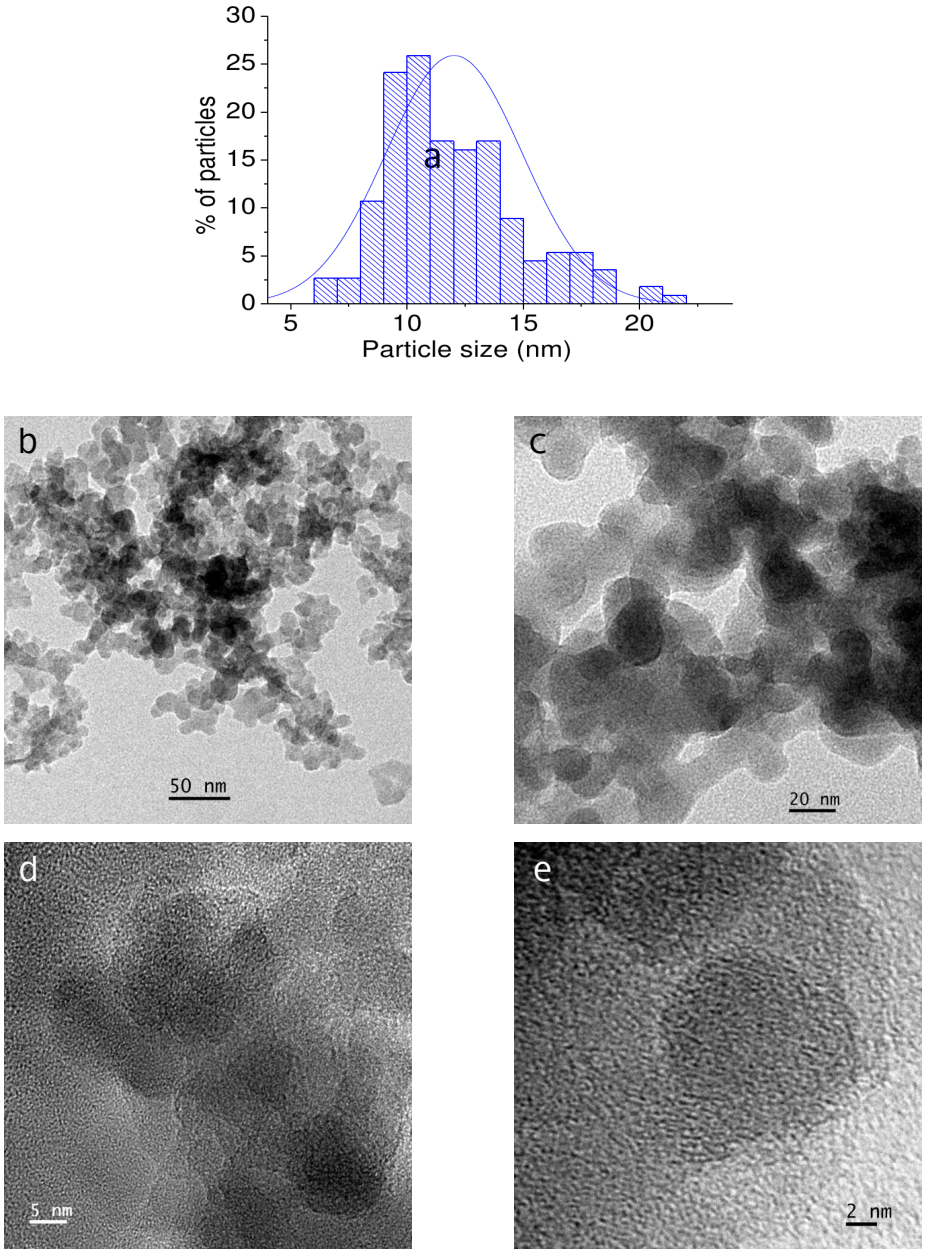

Figure 2: (a)Particle diameter distribution and (b-e) HRTEM images of the Aerosil 300 sample after ~~ALD~~ **coating**.

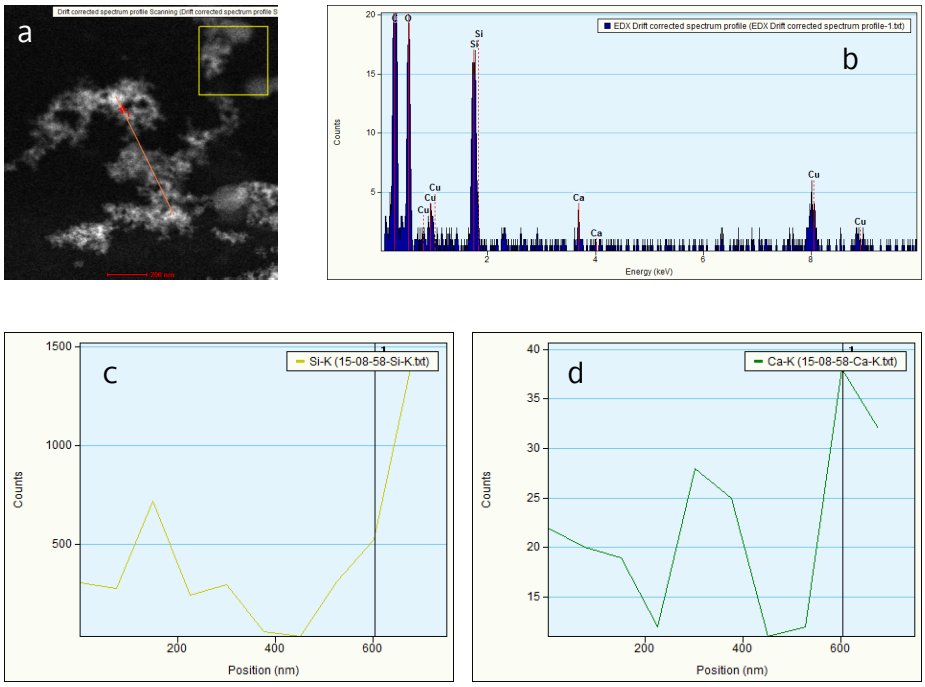

Figure 3: EDX HAADF-STEM results of the Aerosil 300 with ten ~~ALD~~ **coating** cycles sample (a) Drift corrected spectrum profile scanning image, (b) EDX spectrum corresponding to the red cross in the red line profile. (c-d) amounts of Ca and Si along the line profile respectively. Similar results are obtained with the samples based on Aerosil R974.

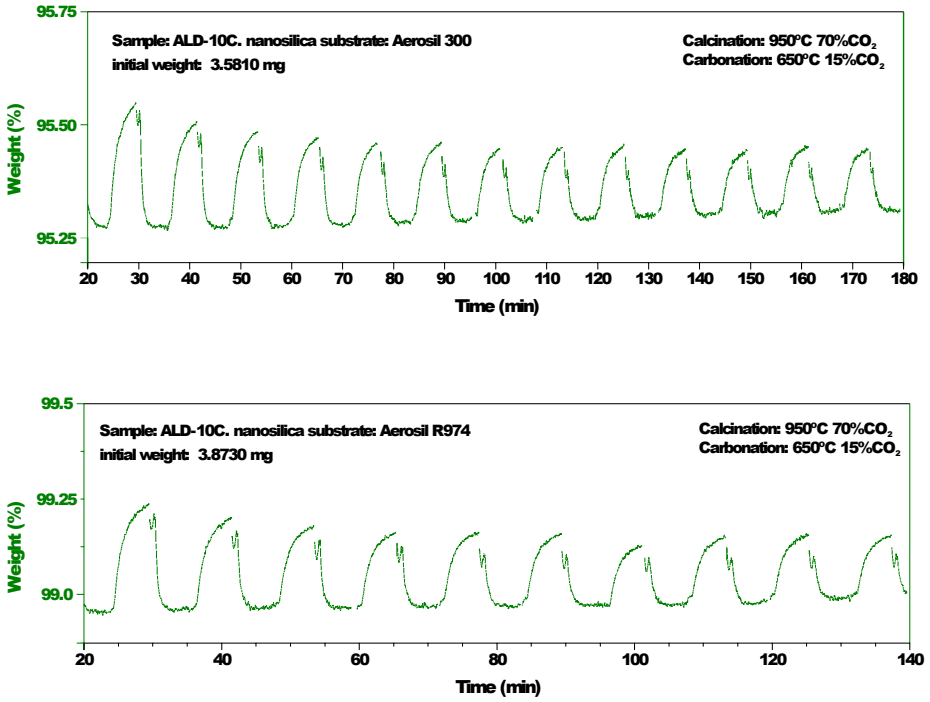

Figure 4: Results of the thermogravimetric analysis of nanosilica layered with CaO ~~by atomic layer deposition~~. Carbonation/calcination conditions are indicated in the insets.